

Supporting Information

Plasmonic Pd-nanoparticles at the Electrode-Semiconductor Interface Enhance the Activity of Bismuth Vanadate for Solar-Driven Glycerol Oxidation

Junjie Xie¹, Brian Tam^{1,2}, YiChao Cai², Longren Li², Zhipeng Lin², Kaat Lambrecht², Artem Bakulin^{1,2*}, Andreas Kafizas^{1,2*}

¹ Centre for Processable Electronics, Imperial College London

² Department of Chemistry, Imperial College London

*co-corresponding authors: a.bakulin@imperial.ac.uk and a.kafizas@imperial.ac.uk

Section S1. Supplementary Figures and Tables

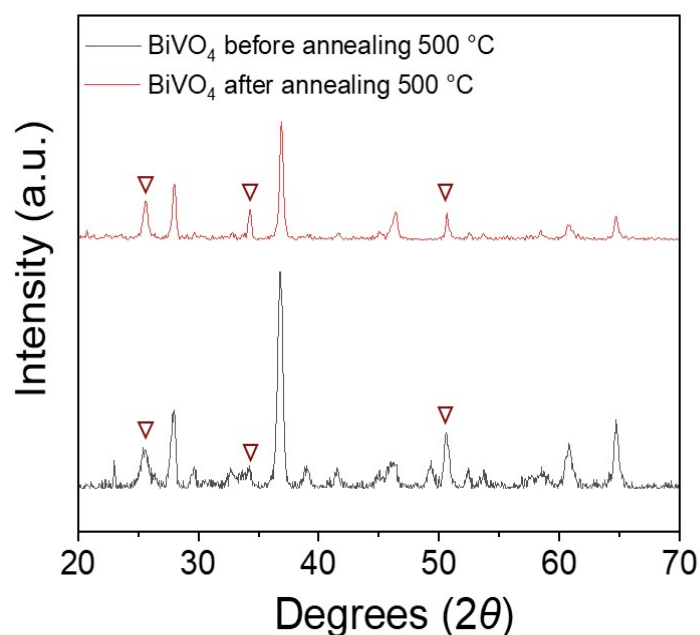


Figure S1. XRD patterns of BVO-coated Pd from 2 mg precursor before and after annealing in air at 500 °C for 2 hours.

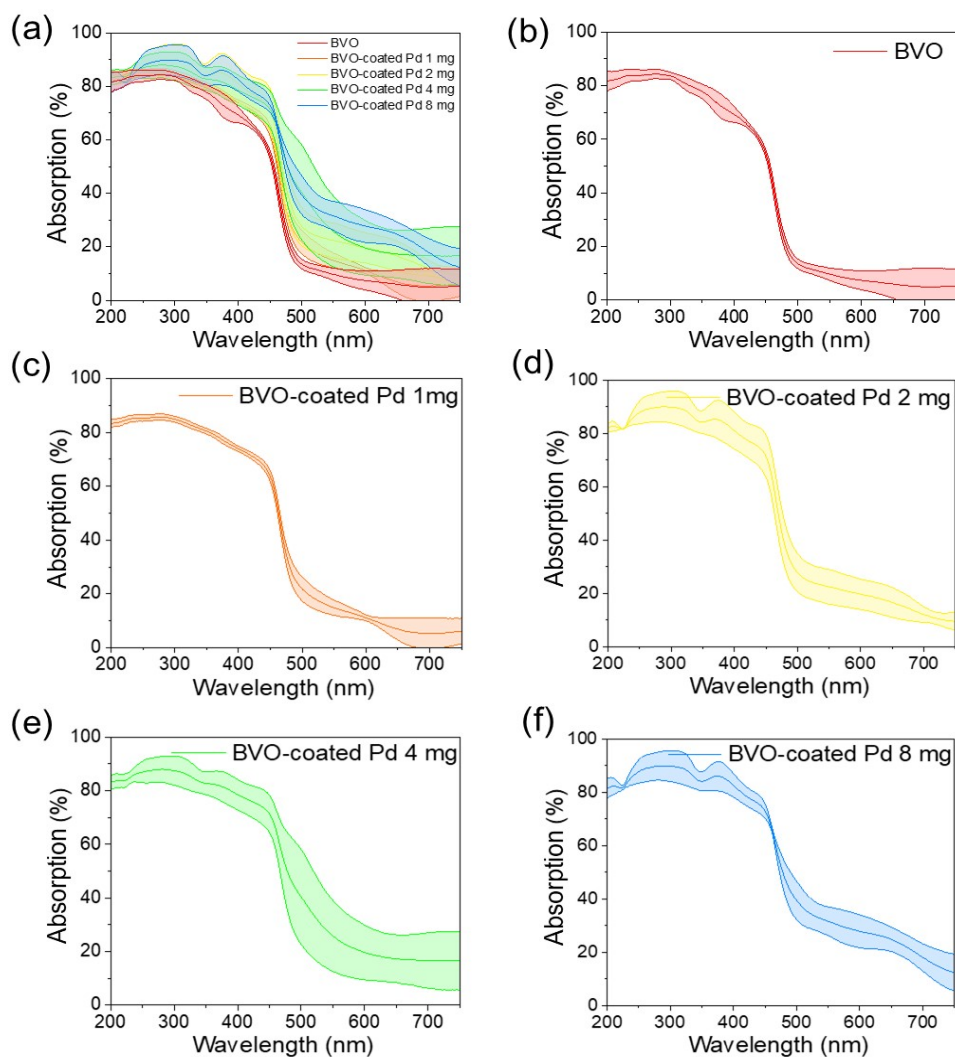


Figure S2. Average absorbance spectra of (a) all BVO and BVO-coated Pd samples with various loadings with three samples used to produce each average and (b) BVO, (c) BVO-coated Pd from 1 mg precursor, (d) BVO-coated Pd from 2 mg precursor, (e) BVO-coated Pd from 4 mg precursor, (f) BVO-coated Pd from 8 mg precursor. The corresponding area for each line is the standard deviation 1σ for each data point.

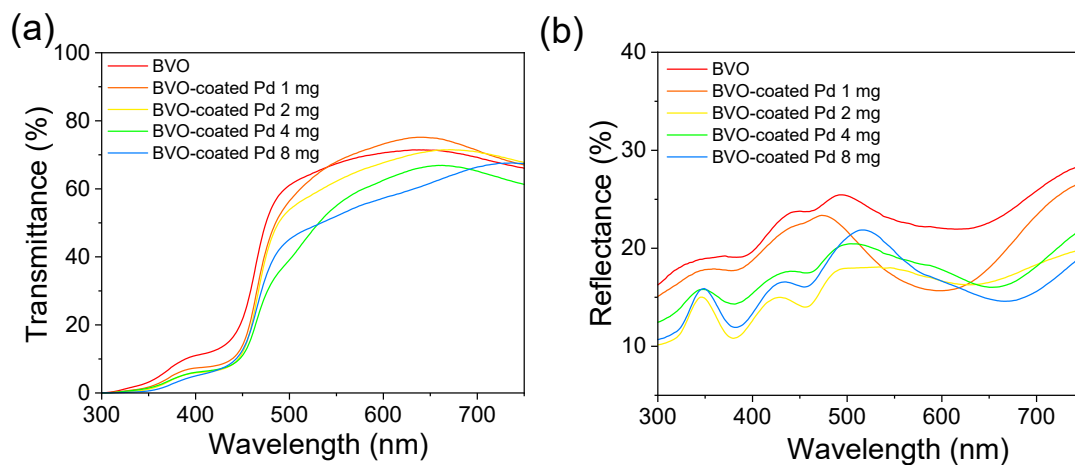


Figure S3. (a) Transmittance and (b) Total reflectance spectra of BVO-coated Pd samples with different precursor masses (X mg, $X=1, 2, 4, 8$) and BVO.

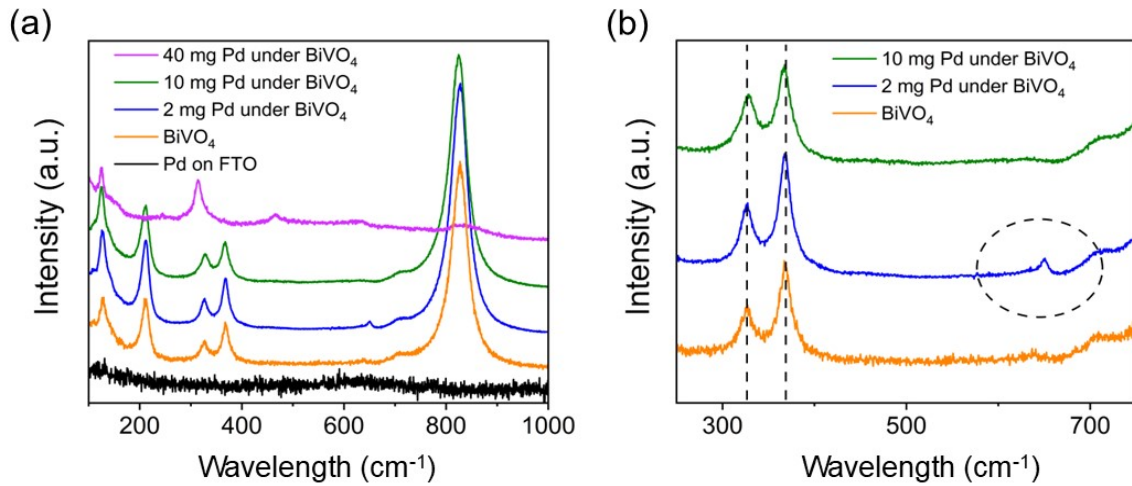


Figure S4. Raman measurements of BVO, Pd on FTO and Pd on BVO samples. (a) Raman spectra of coatings deposited from 2, 10, and 40 mg of Pd precursor under 200 nm BVO compared to the spectra for Pd and BVO on FTO. (b) Raman spectra of coatings deposited from 2 and 10 mg of Pd precursor under 200 nm BVO compared to the spectra for BVO on FTO, zoomed in between 250 to 750 cm⁻¹. Conditions: 532 nm green laser operating at 10% laser power, within 50 to 1000 cm⁻¹ wavenumbers and a resolution of 0.52 cm⁻¹.

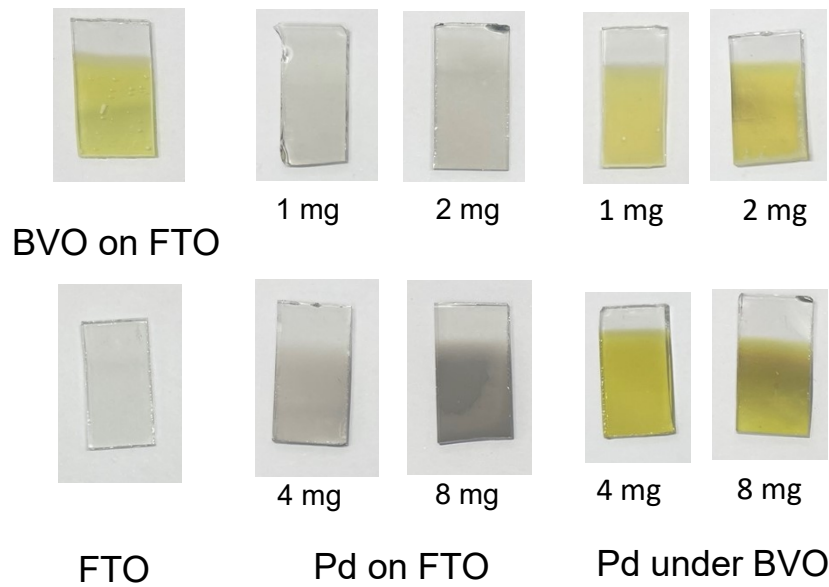


Figure S5. Photos of FTO (1.3 cm x 2.5 cm substrates), bismuth vanadate on FTO (BVO) samples and Pd on FTO, bismuth vanadate on Pd on FTO (BVO-coated Pd) prepared with different amounts of precursor.

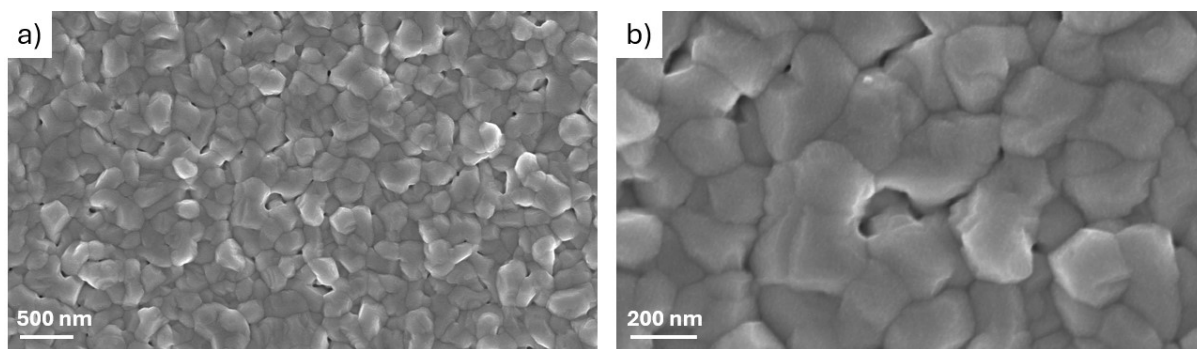


Figure S6. Top-down SEM images of BVO-coated Pd 8 mg (a) at a magnification of 50k x. (b) at a magnification of 150k x.

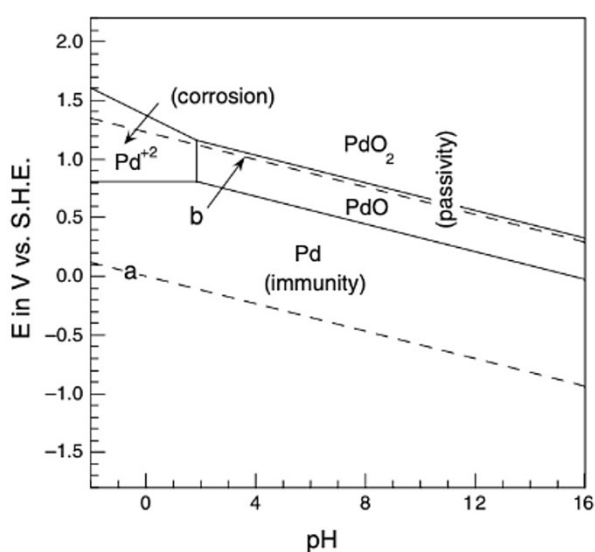


Figure S7. Pourbaix diagram of palladium.¹

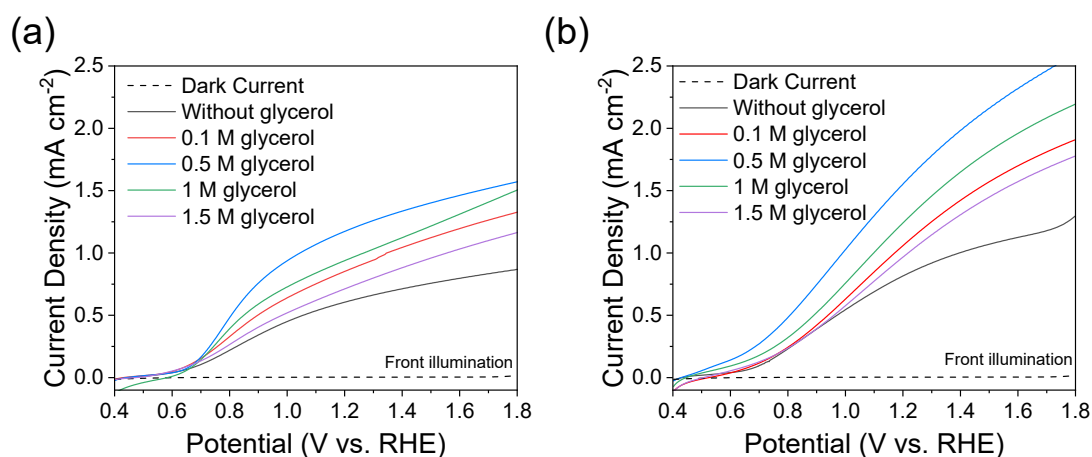


Figure S8. Forward scanning LSV measurement of (a) BVO, and (b) BVO-coated Pd from 4 mg precursor. Conditions: Front illumination, Electrolyte 0.5 M Na_2SO_4 (aq) + 0.1M $\text{K}_2\text{HPO}_4/\text{KH}_2\text{PO}_4$ with the addition of varying concentrations of glycerol, pH 7, under illumination calibrated to 1 simulated sun conditions (Xe lamp, KG3 filter, 100 mW cm^{-2}), Scan rate: 25 mV/s

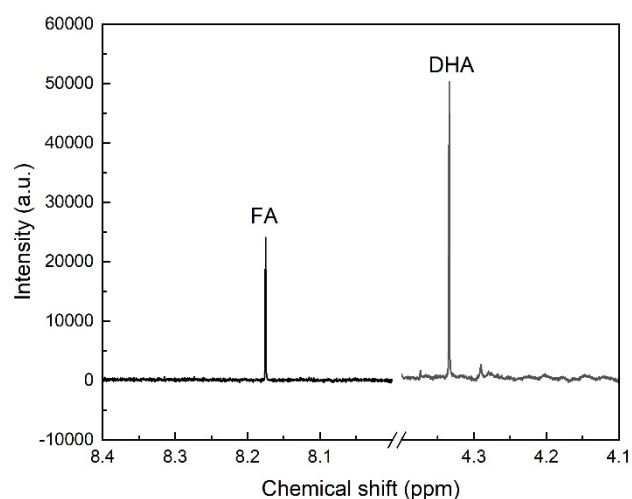


Figure S9. An example ^1H NMR spectrum of an aliquot from the electrolyte of a BVO sample after a chronoamperometry test at an applied voltage of $1.23 V_{\text{RHE}}$ with 0.5 M glycerol. Conditions: Front illumination, Electrolyte 0.5 M Na_2SO_4 (aq) + 0.1M $\text{K}_2\text{HPO}_4/\text{KH}_2\text{PO}_4$, pH 7, under illumination with a 75 W Xe lamp with a KG3 filter set to match the intensity, 100 mW cm^{-2} of 1 sun condition. The ^1H NMR spectrum was acquired in D_2O solvent using a Bruker 400 MHz spectrometer. Quantification of dihydroxyacetone (DHA) and formic acid (FA) concentrations was performed by peak integration with correction for equivalent protons (1 H for FA; 4 H for DHA).

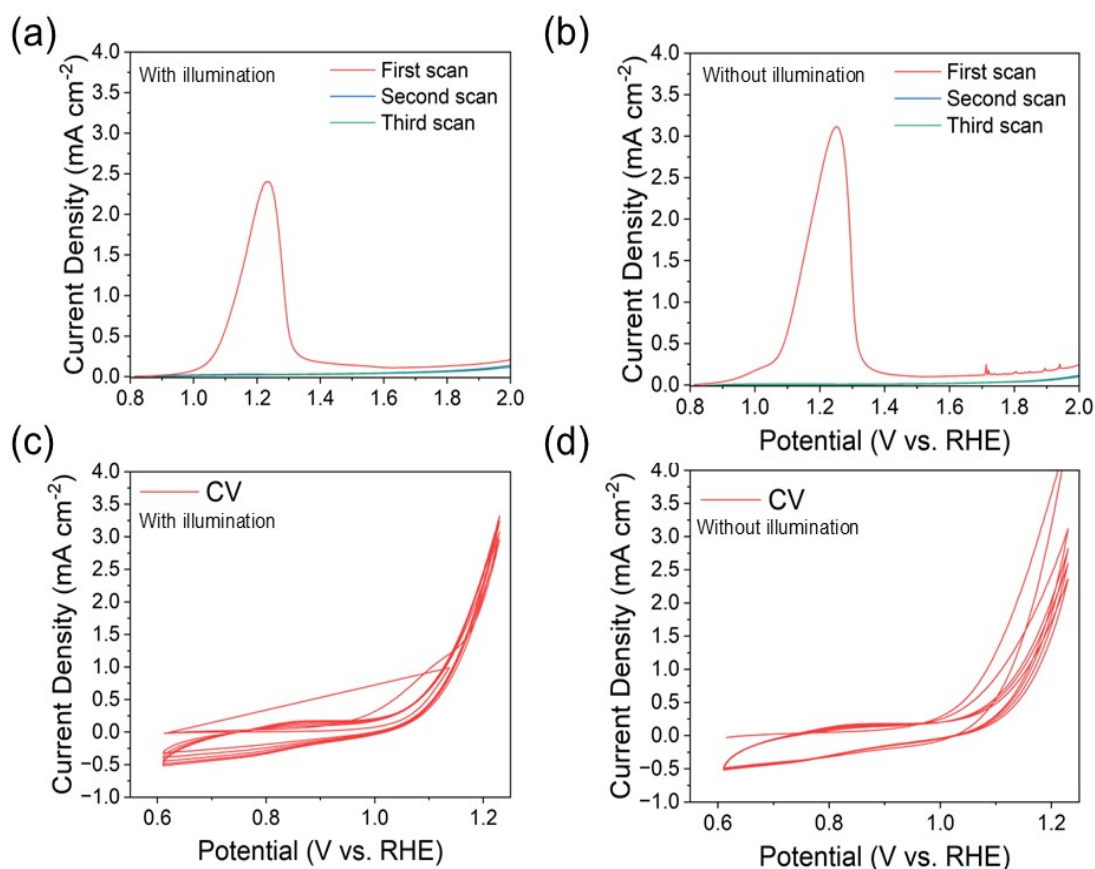


Figure S10. LSV measurements of BVO and Pd on FTO 2mg (a) under front illumination. and (b) without illumination. CV scan of BVO and Pd on BVO 2mg (c) under front illumination. and (d) without illumination. Conditions: Electrolyte 0.5 M Na_2SO_4 (aq) + 0.1M $\text{K}_2\text{HPO}_4/\text{KH}_2\text{PO}_4$, pH 7, under illumination calibrated to 1 simulated sun condition (Xe lamp, KG3 filter, 100 mW cm^{-2}), Scan rate: 25 mV/s .

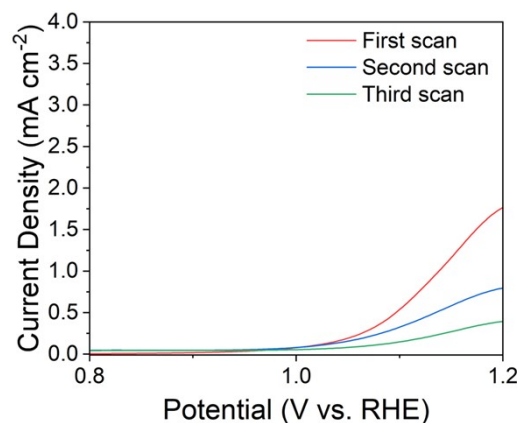


Figure S11. LSV measurements of BVO and Pd on BVO 2mg under front illumination. Conditions: Electrolyte 0.5 M Na_2SO_4 (aq) + 0.1M $\text{K}_2\text{HPO}_4/\text{KH}_2\text{PO}_4$, pH 7, under illumination calibrated to 1 simulated sun condition (Xe lamp, KG3 filter, 100 mW cm^{-2}), Scan rate: 25 mV/s .

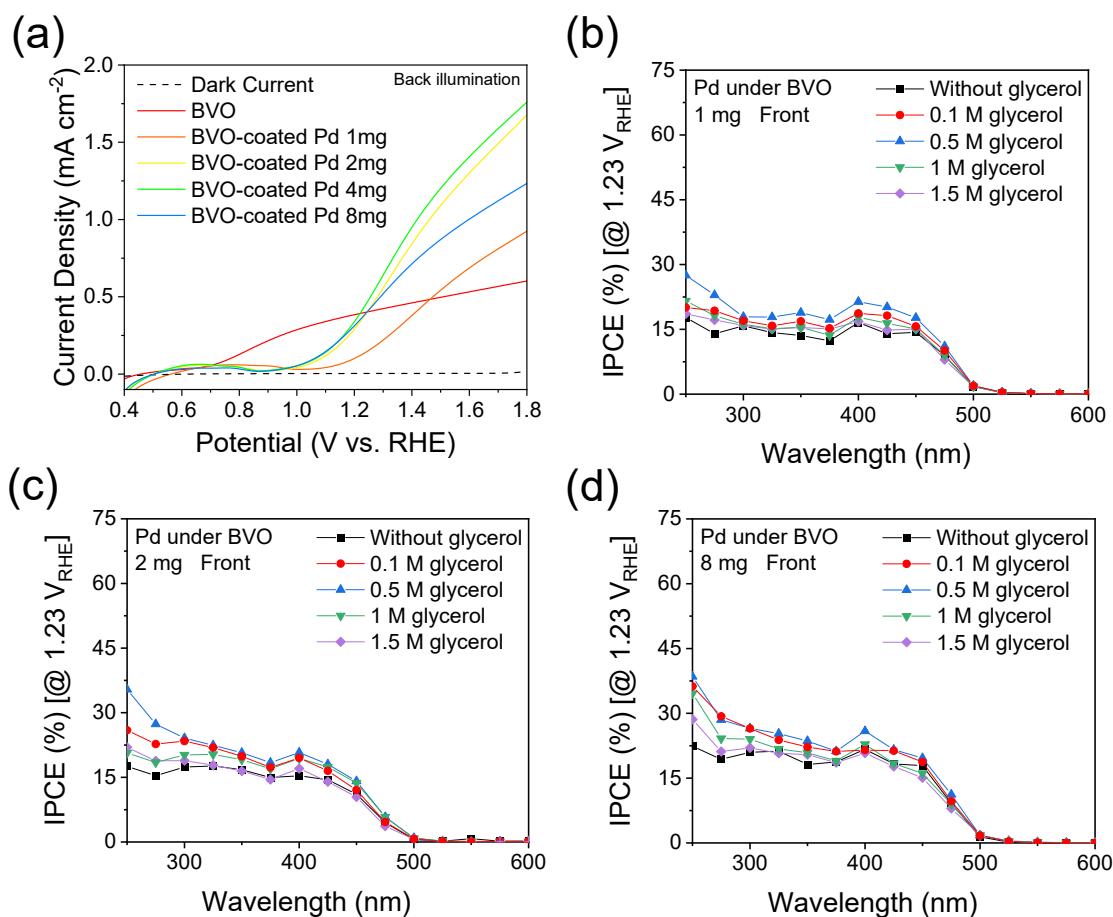


Figure S12. (a) LSV measurement of BVO and BVO-coated Pd samples under back illumination. IPCE spectra of (b) BVO-coated Pd from 1 mg precursor, (c) BVO-coated Pd from 2 mg precursor, (d) BVO-coated Pd from 8 mg precursor comparing with and without the addition of 0.1, 0.5, 1.0 and 1.5 M glycerol, measured at 1.23 V_{RHE} . Conditions: Electrolyte 0.5 M $Na_2SO_4(aq)$ + 0.1M K_2HPO_4/KH_2PO_4 with different concentration of glycerol, pH 7, under illumination calibrated to 1 simulated sun condition (Xe lamp, KG3 filter, 100 mW cm⁻²), Scan rate: 25 mV/s

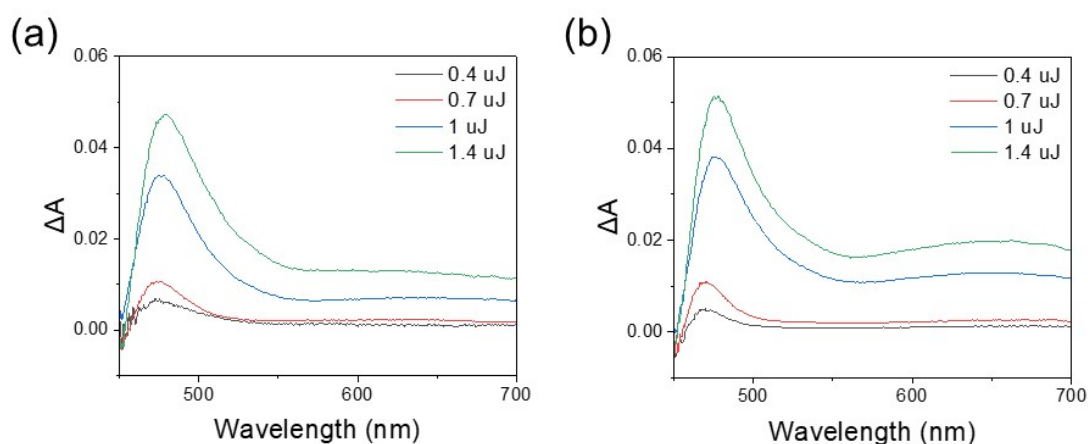


Figure S13. Power-dependent transient absorption spectra at different timescales for (a) BVO in an N_2 atmosphere and (b) BVO-coated Pd from 4 mg precursor in an N_2 atmosphere measured with a 400 nm pump with power of 0.4, 0.7, 1.0, and 1.4 μJ and visible probe from 450 to 700 nm at a time scale of 1 ps after the laser pulse.

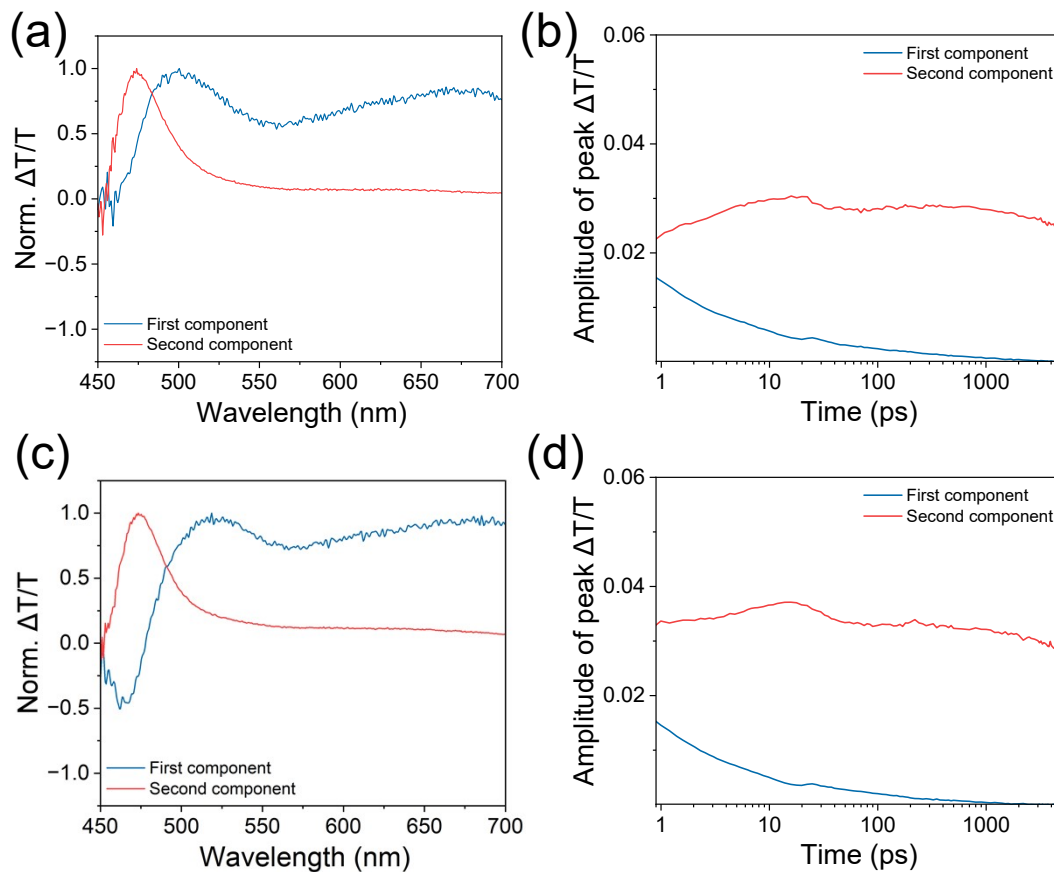


Figure S14. Global analysis of simulated transient absorbance data from a two-compartment model. (a) Time gated spectra and (b) decay traces of BVO-coated Pd from 8 mg precursor. (c) Time gated spectra and (d) decay traces of BVO-coated Pd from 20 mg precursor.

Section S2. Data Fitting for Transient Absorption Spectrum

Exponential decay fitting

The decay kinetics of transient absorption signals were analysed using a biexponential fitting function. This approach assumes that multiple decay channels contribute to the signal relaxation over time. The decay behaviour was modelled by the following equation:

$$\Delta A(t) = A_1 \exp\left(-\frac{t}{\tau_1}\right) + A_2 \exp\left(-\frac{t}{\tau_2}\right) + y_0$$

where A_1 and A_2 are the amplitudes, τ_1 and τ_2 are the characteristic lifetimes of different photophysical processes, and y_0 is the baseline offset. This fitting method enables the extraction of distinct charge carrier dynamics such as fast relaxation and longer-lived recombination or trapping

events, and A_2 are the amplitudes, τ_1 and τ_2 are the characteristic lifetimes of different photophysical processes, and y_0 is the baseline offset. This fitting method enables the extraction of distinct charge carrier dynamics such as fast relaxation and longer-lived recombination or trapping events.

Global Analysis Method

To extract meaningful kinetic and spectral components from time-resolved transient absorption spectra, we employed a global analysis (GA) approach based on a Genetic Algorithm (GAros), which allows for model-free decomposition of complex kinetic data. This method does not rely on predefined kinetic schemes and is especially suitable when the number and nature of intermediate species are not known *a priori*.²

The transient absorption (TA) signal is described as a linear combination of species-associated spectra and their corresponding time-dependent populations:

$$\Delta A(t, \lambda) = \sum_{i=1}^2 c_i(t) \cdot e_i(\lambda)$$

Here, $\Delta A(t, \lambda)$ is the experimental TA data matrix, $c_i(t)$ are the time-dependent concentrations (or amplitudes) of species i , and $e_i(\lambda)$ are their associated spectra. $\Delta A(t, \lambda)$ is the experimental TA data matrix, $c_i(t)$ are the time-dependent concentrations (or amplitudes) of species i , and $e_i(\lambda)$ are their associated spectra. The GA-based global analysis mimics the process of natural selection. A population of candidate spectral components (representing different possible species) is generated by introducing stochastic noise and random Gaussian features onto initial guesses. Each candidate's fitness is evaluated by how well it reconstructs the measured TA data. A fitness function f is defined as the inverse of the mean squared residuals, optionally penalized by spectral or kinetic constraints (e.g. non-negativity). f is defined as the inverse of the mean squared residuals, optionally penalized by spectral or kinetic constraints (e.g. non-negativity):

$$f = \left(\frac{(TA - T^{\wedge}A)^2}{unc} \right) \times \left(1 + nkp \cdot \frac{N_{neg}}{N_{tot}} \right)^{-1}$$

where $T^{\wedge}A = tt \times npe$, and tt are time traces computed by least-squares inversion of TA data with respect to spectra spe . $tt = tt \cdot npe$, and tt are time traces computed by least-squares inversion of TA data with respect to spectra spe . The GA iteratively optimizes the spectra through selection, crossover, and mutation of spectral candidates. Spectral sign constraints (positive for GSB/SE, negative for PIA) are enforced during the mutation steps to reflect known photophysical behaviour. To enhance computational efficiency and minimize overfitting to noise, the data are smoothed and wavelength-subsampled prior to fitting. To enhance computational efficiency and minimize overfitting to noise, the data are smoothed and wavelength-subsampled prior to fitting.

The choice of using two components was based on both physical interpretability and comparative fitting tests. As shown in Supplementary **Figure S16**, applying a three-component fit resulted in significant spectral and kinetic overlap between the second and third components, indicating redundancy rather than additional mechanistic insight. Therefore, the two-component solution was adopted as the simplest and most robust representation of the underlying dynamics.

The decision to use two components was based on the convergence of residuals and the physical interpretability of the extracted spectra. Increasing the number of components beyond two did not yield independent or meaningful features and introduced instability in the fitting results.

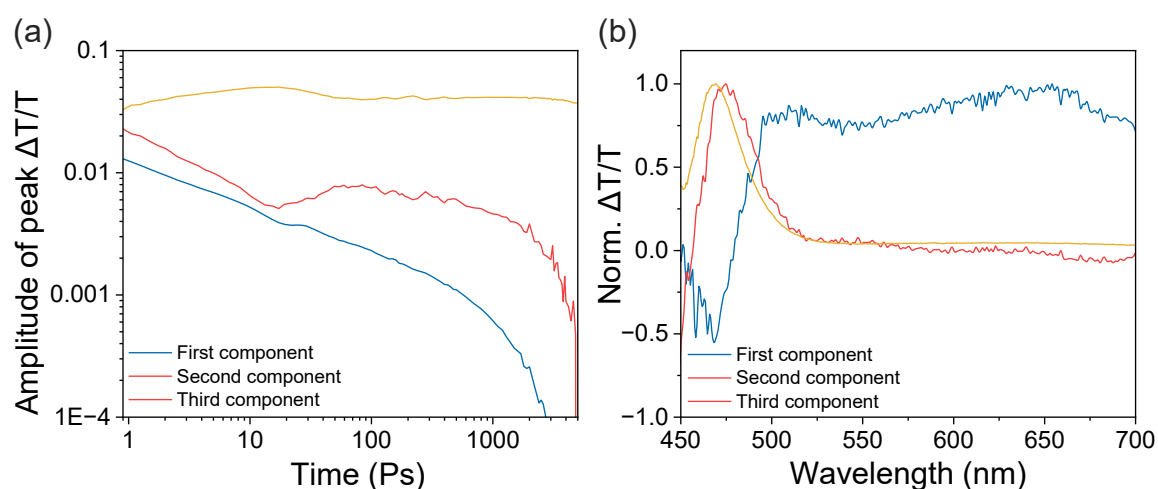


Figure S15. (a) The species associated spectra (SAS) and (b) decay traces of BVO-coated Pd from 4 mg precursor with the three resolved components shown.

References

1. Bard, A., Standard Potentials in Aqueous Solution (1st ed.). Routledge: 2017. <https://doi.org/https://doi.org/10.1201/9780203738764>
2. Van Stokkum, I. H.; Larsen, D. S.; Van Grondelle, R., Global and target analysis of time-resolved spectra. *Biochimica et Biophysica Acta (BBA)-Bioenergetics* **2004**, 1657 (2-3), 82-104.